

Experimental Characterization and Control of Miniaturized Pneumatic Artificial Muscle

Shanthanu Chakravarthy, Aditya K. and Ashitava Ghosal
Department of Mechanical Engineering
Indian Institute of Science
Bangalore, India
{sc, adityak, asitava}@mecheng.iisc.ernet.in

Abstract— Robotic surgical tools used in minimally invasive surgeries (MIS) require miniaturized and reliable actuators for precise positioning and control of the end-effector. Miniature pneumatic artificial muscles (MPAM) are a good choice due to their inert nature, high force to weight ratio and fast actuation. In this paper, we present the development of a miniaturized braided pneumatic muscles with an outer diameter of ~ 1.2 mm, a high contraction ratio of about 18% and capable of providing a pull force in excess of 4 N at a supply pressure of 0.8 MPa. We present the details of the developed experimental setup, experimental data on contraction and force as a function of applied pressure, and characterization of the MPAM. We also present a simple kinematics and experimental data based model of the braided pneumatic muscle and show that the model predicts contraction in length to within 20% of the measured value. Finally, a robust controller for the MPAMs is developed and validated with experiments and it is shown that the MPAMs have a time constant of ~ 10 ms thereby making them suitable for actuating endoscopic and robotic surgical tools.

Keywords — *Artificial pneumatic muscles, miniaturized actuators, minimally invasive surgery tools, pneumatic actuator control.*

I. INTRODUCTION

Minimally invasive surgeries (MIS) with its advantages of low blood loss, less exposure to external pathogens, faster recovery and less trauma are being increasingly used by surgeons and there is a need to develop new surgical devices and tools for MIS procedures [1]. One of the key challenges in developing such devices is the requirement of micro actuators which can work *in-vivo* and with capability of precise positioning and control. Pneumatic artificial muscles (PAM) are soft actuators that generate contraction forces with desirable properties such as compliance, robustness, biological inertness and these make them suitable for in-vivo operation [2-5]. The conventional PAM's such as those used for robotic and industrial applications are difficult to integrate with MIS tools as they are too large and require

high pressure for their operation. In this work we present miniature pneumatic artificial muscles (MPAM) that have a diameter of only 1.2 mm and are suitable for use in minimally invasive surgeries. Although pneumatic artificial muscles have many advantages they have non-linear characteristics and pose considerable challenge in their modeling and control. In this work we present experimental characterization, a purely kinematic based modeling, and non-linear control of the developed MPAMs.

Extensive use of minimally invasive surgeries such as natural orifice transluminal endoscopic surgery (NOTES) are being limited due to the non-availability of dexterous surgical devices that are simple to use. Existing diagnostic devices such as endoscopes are actuated by wires making them flexible and this makes them difficult for precise positioning of end-effectors used for biopsy or other minute surgical procedures. A way to overcome this problem is to develop mechanisms which are flexible and at the same time can be made stiff to precisely position the end-effectors. This, however, require the use of miniature actuators and several attempts were made by researchers in developing the micro actuators for surgical tool applications. Ikuta et al. developed segmented active endoscope actuated with shape memory alloy (SMA) servo actuators [6]. However, this actuator required high currents and the actuation was slow. Simaan et al.[7] also developed a four-degrees-of-freedom snake like robot actuated by SMA wires. The laboratorie de Robotique de Paris (LRP) developed a 8 mm in diameter snake like mechanism, formed by a sequence of segments and articulated by SMA actuated pin joints [8]. Choset [9] developed a design with two concentric tubes consisting of a series of cylindrical links connected by spherical joints. In this design the joints cannot be actuated independently and slow forward speed and large external feeding mechanism is required. Grundfest et al. [10] developed a macroscopic version of an active endoscope driven by wires. Webster et al. developed continuum robot based on pre-curved tubes. These robots used active cannulas that are composed of super-elastic component tubes that can extend telescopically and rotate axially [11]. Scientists from Imperial College, London used miniature motors together with tendons that have complex assembly to develop prototype articulated snake like robot [12]. Researchers from SRI International have also developed electro-strictive polymer artificial muscle (EPAM) and proved that its specific power is comparable to that of an electric motors [13]. They also developed a serpentine manipulator using a spherical joint actuated by EPAM. A. Moers et al. [14]] reported their work on surgical device using micro hydraulic cylinders and they presented the complete design and control of their micro hydraulic cylinder for use in surgical instrument.

Most designs discussed above take advantage of SMA or cable actuation to design slender surgical devices. Stiffness cannot be easily controlled in cable actuation and the driving unit is complex and involves issues of friction. SMA actuation is slow and requires high activation voltage. Electro active polymers are expensive and difficult to manufacture and pose considerable complexity in their control and use of miniature motors results in complex transmission requirements. Considering all these factors miniature-PAMs with their active variable-stiffness, flexibility, low cost of manufacturing, and high force to weight ratio emerge as a promising micro actuator for use in miniature surgical tools. In this work, the development, characterization, modeling and control of MPAM as an actuator for use in surgical tools is presented.

Conventional PAMs have been in existence since 1950s and different forms of PAMs have been commercialized by several companies such as Bridgestone, Festo Corporation and Shadow Robot. However, modeling and control of these actuators is non-trivial due to complex physical interactions that happen during the actuation of the pneumatic muscle. Analytical modeling using principle of virtual work and modeling in a continuum approach are the two main trends seen in the literature of pneumatic muscle modeling (see the review paper by Tondu et al. [15].) The virtual work principle was applied by Chou and Hannaford [2] for modeling commercial PAMs. Many modifications and improvements have been added on the original model to better capture the force contraction relation seen in experiments [4, 16]. Liu and Rahn formulated the pneumatic muscle contraction in the continuum framework [17]. They modeled the PAM as a fiber-reinforced membrane and simplified the problem by considering symmetry. Finite element analysis (FEA) based models are also seen in literature [18, 19]. However, these models have many inherent assumptions, inaccurate and cannot be used in real-time control. Analytical solutions that model the pneumatic model are simple, derived using many assumptions and do not capture all the physical behavior observed in experiments. The suggested analytical models have a fitting parameter that is estimated based on experiments and varies with input [4]. Continuum based models are computationally expensive, complex, and in many cases the numerical scheme used for computation may not converge to a solution. This complexity involved with continuum approach renders the model impractical to be used in design and control. As an alternative to these modeling techniques, in this work we present an experiment based model using only the braid kinematics (and ignoring elasticity of the components of the MPAM) and show that

the model prediction deviate less than 20% from experimental observations. Furthermore, we present and analyze the factors that cause the deviation of the model from the actual behavior of MPAMs.

Linear control strategy has been used by researchers to control miniature pneumatic muscles [4]. In these works custom valves for controlling the pressure in the pneumatic circuit are developed. Linear controller was only effective for a particular operational region and required a time of 3 s to achieve desired position [3]. Nonlinear control strategies provide robust and more accurate control of PAMs [20, 21] as compared to linear control. However, the performance of most of the nonlinear control strategies depends on the accuracy of dynamic model. In this paper we present error based sliding mode technique for control of MPAMs. We develop the instrumentation and electronics required for feedback control of MPAMs and validate the proposed controller experimentally. Our experiments show that the implemented sliding mode controller is robust against uncertainties and the response times are of the order of 10 ms.

This paper is organized as follows: in the next section, we present the details and the fabrication of the MPAMs. In section 3, we present experimental results for characterizing the MPAMs and a purely kinematic model for the braided MPAMs. In section 4 we present the details of a controller for the MPAMs and in section 5, we present a design and initial experiments with a surgical tool based on the developed MPAMS. In section 6, we present the conclusions.

II. FABRICATION OF MINIATURIZED PNEUMATIC ARTIFICIAL MUSCLE (MPAM)

Pneumatic muscle possesses intriguing behavior that converts pneumatic energy into mechanical energy by transforming the pressure applied into the physical contraction of the muscle. As shown in Fig. 1 a soft, stretchable inner silicone tube and the outer braided nylon sleeve are the two important components that make a pneumatic muscle. The inner silicone tube expands more than 100% when pressurized and the outer braid cannot hold pressurized air and has a geometric arrangement that contracts when radially stretched. However, when silicone tube and outer braid is arranged and pressurized, the PAM contracts. The contraction of the PAM is similar to a biological muscle and hence the name muscle is attached to the actuator. Silicone tube adds stiffness to the PAM and helps to confine the pressurized air. The outer braided mesh constrains the inflation of the pressurized silicone tube and prevents its rupture. It also converts large radial expansion into axial contraction due to its geometrical arrangement and helps set limits of contraction.

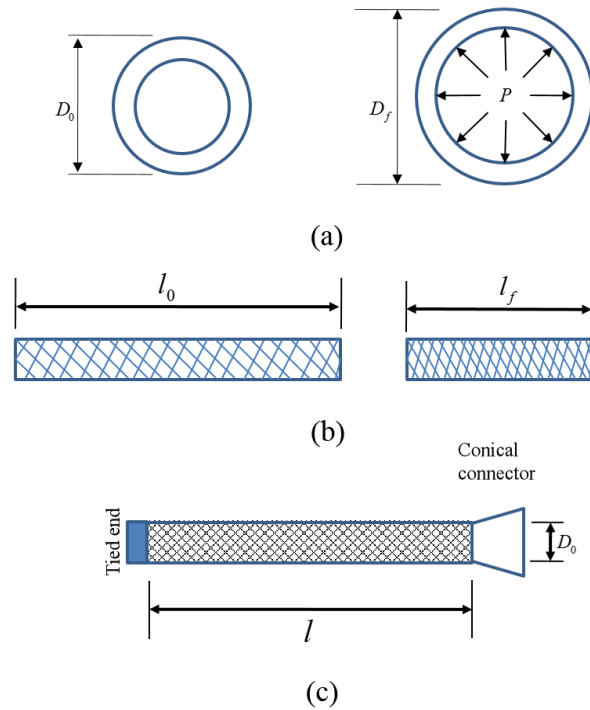


Fig.1: (a) Un-pressurized (left) and pressurized (right) cross-section of the silicone tube, (b) Initial (left) and contracted length (right) of the braid, and (c) Silicone tube and braid arranged to obtain pneumatic muscle.

The miniaturization of PAM can be achieved by reducing the diameter of the silicone tube. However, reducing the diameter of the silicone tube reduces the contraction and force capacity of the PAM [22]. One way to overcome this problem and achieve miniaturization is by selecting tubes that have low wall thickness. However, choosing lower wall thickness results in lower operating pressures and hence lower contraction are possible. An optimal diameter and wall thickness has to be chosen for developing MPAMs that give sufficient contraction and pull-force. In miniaturizing the pneumatic muscle, we experimented with several different diameters and wall thickness before choosing the dimensions discussed next.

The fabricated MPAM's are made out of platinum cured silicone tube with inner diameter of 0.5 mm and outer diameter of 0.9 mm. Before braiding, the silicone tube is pre-stretched several times by pressurizing the silicone tube and releasing the pressure. This process relieves the bias in the silicone tube and results in uniform expansion of the tube. After this process a nylon mesh is tailored on the pre-stretched silicone tube using a vertical braiding machine. For the braids used in this work, the gear ratio in the braiding machine was set at 1:12. The wire diameter of nylon braided sleeve is ~ 0.1 mm and the braids are weaved to form a pantograph pattern with a braid angle of ~ 20 degrees.

Finally one end of the MPAM is knotted using surgical thread and the other end of the MPAM is attached to a conical connector and wrapped with surgical thread to make it more air-tight. Figure 2 shows the fabricated MPAM. The thickness of the developed MPAM was measured using laser interferometer and is ~ 1.2 mm. Different length MPAM's can be manufactured by varying the length of the silicone tube.

III. CHARACTERIZATION AND MODELING OF MPAM

In this section, we present the characterization and modeling of the fabricated MPAM. Three representative MPAMs, all with outer diameter of 1.2 mm, with lengths of 97 mm, 117 mm, and 143 mm were characterized. It may be noted that the chosen lengths are typical for use in the planned endoscopic surgical device and the experiments presented in the rest of this paper will use the same lengths. We start the characterization of the MPAM by determining the maximum force output capacity of the muscle.

A. Maximum force characterization

To measure the maximum force exerted by the MPAMs, the free end of the MPAM was connected to a commercially available load-cell with a resolution of 1 mN and a maximum saturation force of 5 N. In this arrangement the pneumatic muscle is constrained from contraction and we measure the pull force as a function of the applied pressure. Figure.3 (a) shows the experimental setup used for force characterization. It can be observed from Fig.3 (b) that a pull force of 4.2 N, 3.5 N and 3 N are achieved respectively for the three tested length 97 mm, 117 mm and 143 mm. The curves in Fig.3

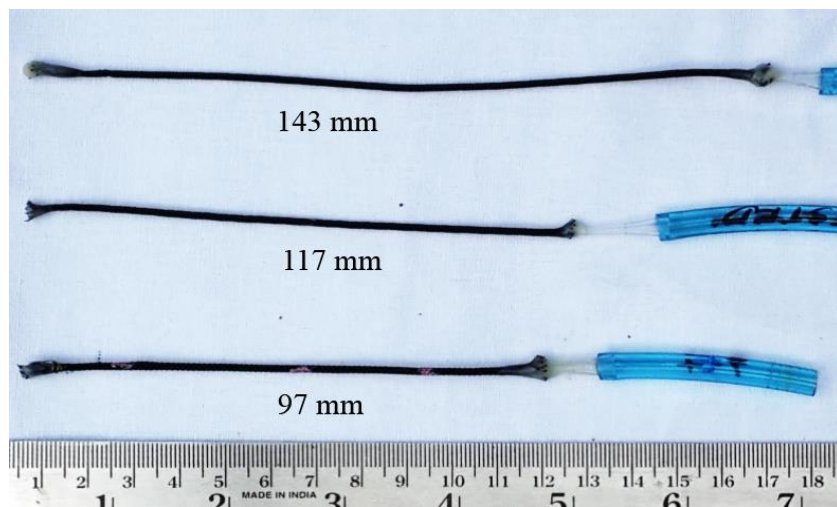


Fig. 2: Fabricated miniaturized pneumatic artificial muscles (MPAM).

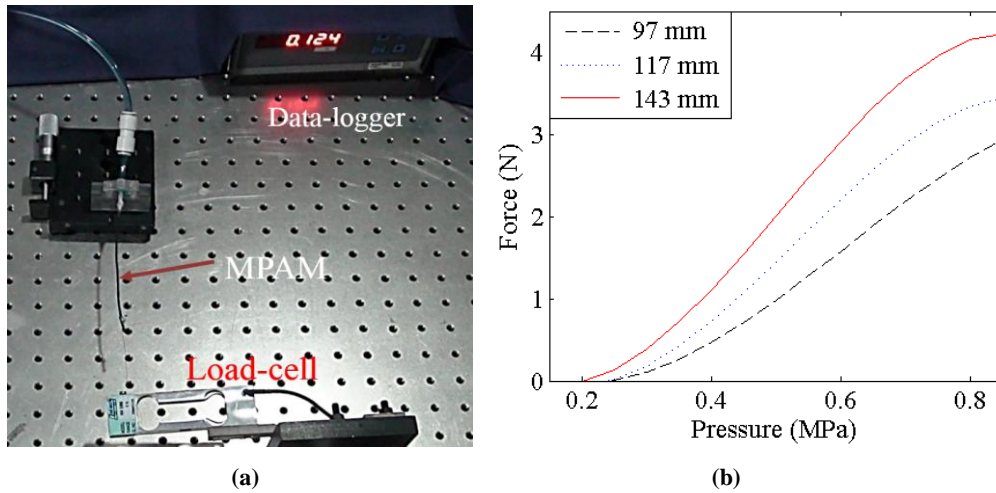


Fig. 3: (a) Experimental setup for obtaining maximum force generated by the MPAM, (b) Forces versus pressure for different lengths of the MPAMs.

(b) was obtained using a cubic fit for the experimental data obtained by measuring static force for every 0.069MPa. These results clearly show that, unlike the claims in [4] the static force capacity is not independent of initial length and increases with increase in initial length of the MPAMs. This maximum force experiment also gives basis for deciding the loading conditions for rest of the characterization.

B. Static characterization of the MPAMs

Apart from force characteristics we are also interested in contraction of the MPAMs since the varying contraction of pneumatic muscle, under various input pressure, is planned to be used for positioning the surgical device. Commercially available PAMs are large and standard Universal Testing Machines (UTM) with air supply can be used for their characterization. The MPAMs developed in this work are miniaturized and require special setup for their characterization. Figure 4 shows the experimental setup developed for static characterization of MPAMs. The experimental setup consists of an air compressor with a maximum output pressure of 1 MPa, a reservoir, timing belt and pulley arrangement. The reservoir in the pneumatic circuit removes fluctuation in pressure and helps in smooth contraction of the muscle. The teeth on the timing belt ensure no slipping happens and the displacement measurements are accurate. Standard weights ranging from 10g to 600 g are used to apply axial loads at the free end for the timing belt. A silicon pressure transducer manufactured by Honeywell (0 to 1 MPa) is used to measure the pressure. An encoder with 500 counts per revolution is attached to the pulley shaft for measuring the displacements. The system has a

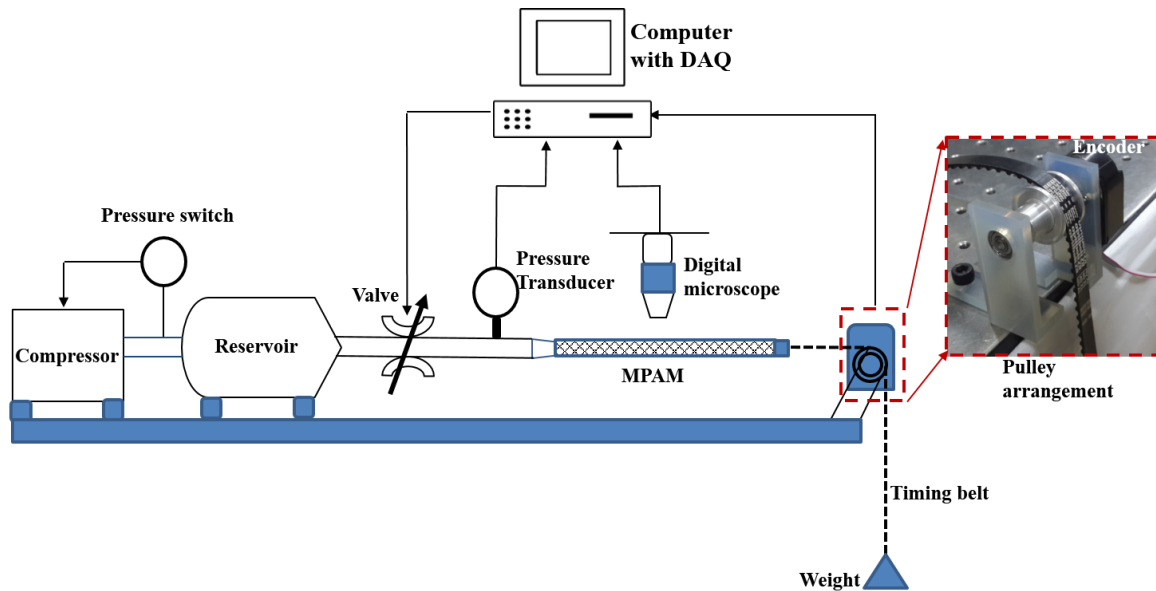


Fig. 4: Experimental setup used for characterizing the MPAMs.

resolution of 0.17 mm for measuring linear displacements. Two proportional valves (VSO series manufactured by Parker Inc) are used to control the pressure by applying voltage to the valves. One of the valves regulates the inlet air flow and is used for inflating the pneumatic muscle and the other valve is used as a bleed valve. A dSPACE 1103 board serves as a data acquisition (DAQ) device for recording data from the pressure transducer and encoder. Data was collected on a computer with the DAQ sampling at 1 kHz.

To obtain contraction and generated force as a function of the applied pressure, a systematic set of experiments were performed with the developed MPAMs. During the experiments, one side of the MPAM is fixed to a block using a clamp and a timing belt is tied to the free end of the pneumatic muscle. The timing belt from the free end of the MPAM is looped around the pulley for hanging weights. Different weights were suspended and the contraction and force generated by the pneumatic muscle are measured for different pressures. Figure 5 shows the experimental results obtained during characterization of the three MPAMs. It can be seen that the behavior of an MPAM, as expected, is not linear. However, a cubic polynomial fits the data for each pressure controlled experiment reasonably well. Numerous experiments were carried out to characterize the MPAMs and the error bars obtained from all the experiments are indicated in Fig 5. It can be seen that the experiments are repeatable with small error bars (maximum standard deviation of 0.003). Experiments show that a maximum contraction of $\sim 18\%$ is achieved at a pressure of 0.82 MPa for a length of 143 mm. Our fabricated MPAMs show good contraction (5% to 20 %) when operated with an input pressure greater

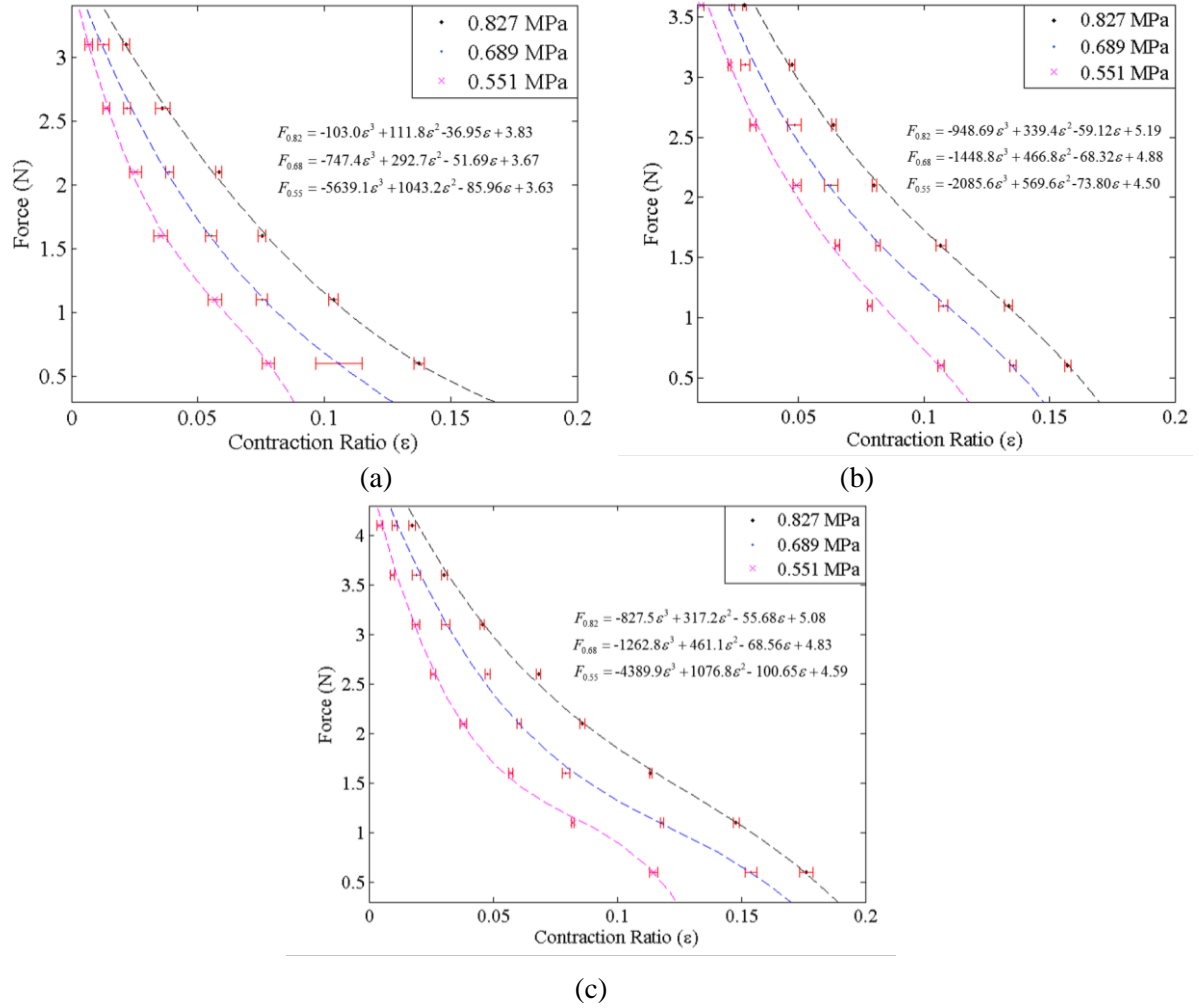


Fig. 5: Force versus contraction plots for lengths (a) 97 mm, (b) 117 mm and (c) 143 mm.

than 0.5 MPa and loading condition below 3 N. The MPAMs contraction reduces to less than 5 % when operated with a load of greater than 3N. During our experiments we also noted more than 25 % contraction when the MPAMs were pressurized to 1 MPa. The results for higher pressures are not shown as the surgical device may become unsafe at higher pressures and we have restricted the operating pressure to 0.8 MPa.

Hysteresis is commonly associated with pneumatic actuators and need to be characterized. The experimental results for the hysteresis behavior of the MPAM are shown in Fig.6 where a third order polynomial is used to fit the behavior. As can be seen in figure, greater pressure is required for contracting the MPAM compared with that required during its extension. This hysteresis behavior is attributed to the friction in the braided shell of the MPAMs and due to the large deformation of the silicone tube. This hysteresis behavior needs to be taken into account and compensated when MPAMs are being used as positioning actuators.

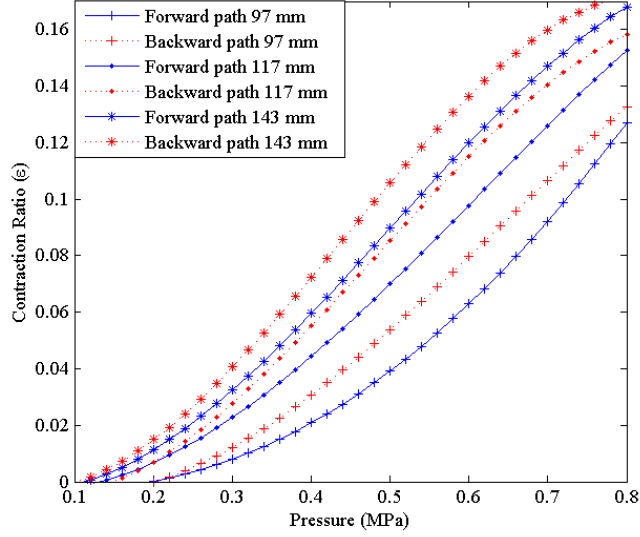


Fig. 6: Hysteresis in the fabricated MPAMs.

C. Kinematic model of an MPAM

One of the goals of the research is to develop reasonably accurate models for MPAMs where the force and contraction can be obtained as a function of the various physical parameters and input pressure thereby obviating the need for resorting to experiments every time. We present a simple kinematic model of the braided silicone tube shown in Fig. 7. The first assumption is that the outer braided shell is infinitely stiff when compared to inner silicone tube and two typical strands of the braid are wrapped around as shown in Fig. 7(a). The length of an inextensible strand is L_s and we assume that all the strands are of equal length. Considering only two strands, we next assume that they form a pantograph mechanism with scissor-like elements [23] with the intersection of the strands acting like a pin joint due to the nature of interweaving in the braid. We further assume that the pantograph mechanism is planar as shown in the right-hand side of Fig. 7(b) and the pantograph structure of the mechanism is retained during contraction of the MPAM. As shown in the figure, one end of the pantograph mechanism is fixed and at the other end a displacement can be applied. It is known in literature [19] that as the length l increases, the angle θ decreases and vice-versa. Similar to a planar pantograph mechanism, we assume that the kinematic relation that relates the braid angle, θ with the length of the pneumatic muscle is given by,

$$l = L_s \cos(\theta) \quad (1)$$

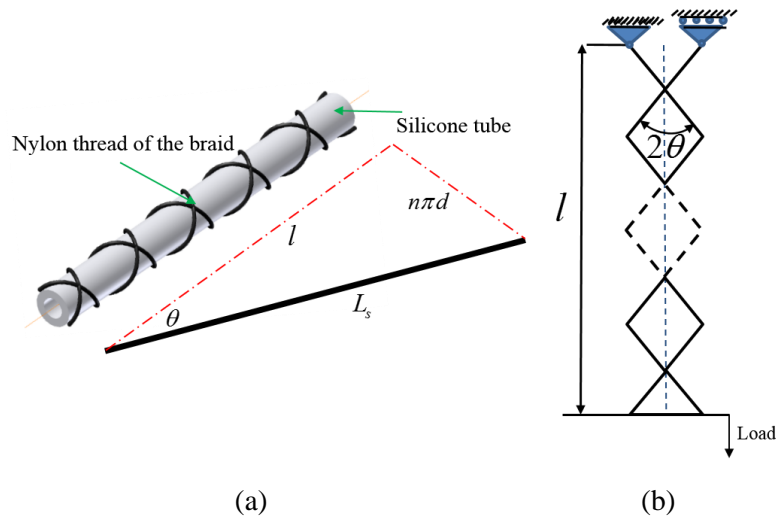


Fig. 7: (a) Geometric representation of the actuator, (b) pantograph representation of the braid.

where l is the length of the pneumatic muscle and L_s is the length of the single strand of the braid assumed to be constant.

Several experiments are carried out to check the validity of the kinematic relation given in (1) using the experimental setup described in Section 3. We used three different external loading conditions based on the maximum force experiment described earlier. The loading conditions are chosen to be distributed with one closer to the lower and upper end and one representing the middle of the range. Three different MPAMs of initial lengths of 97 mm, 117 mm and 145 mm, were pressurized to different pressures and the contracted length for input pressure and loading were measured. A digital microscope was used for capturing photographs of the MPAMs and the braid angle of the MPAM at the center of the MPAM was measured for each pressure and loading [24]. It may be noted that at the ends the braid angle is different from that at the center (see figure 8a and 8b) but the end-effect may not be large for the length of the muscle

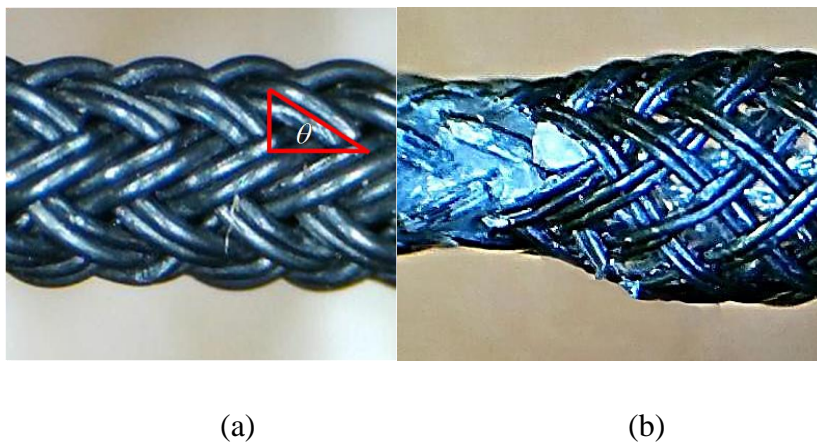


Fig. 8: Magnified view of the (a) central and (b) end section of the braid captured using digital microscope.

tested here [15]. After the complete set of experiments, the length of a single strand in each of the MPAMs was measured and L_s was determined.

Figure 9 shows the plot of (contracted) length versus cosine of the braid angle for the three different MPAMs. It may be noted that the resolution of angle measurement is ± 1 degree and the standard deviation of the error in length measurement is about 0.8 mm. These are shown as error bars in Fig. 9. A linear fit is done on the experimental data and based on the fit, the length, l and cosine of the braid angle relation can be expressed as,

$$l = (L_s \cos(\theta)) k_1 + k_2 \quad (2)$$

where L_s , k_1 and k_2 are the slope and intercept. Table 1 presents the values of k_1 and k_2 for each of the MPAMs whose nominal (un-pressurized) length and strand lengths L_s are given in column 1 and 2, respectively. We can make the following observations from the results presented in Table 1.

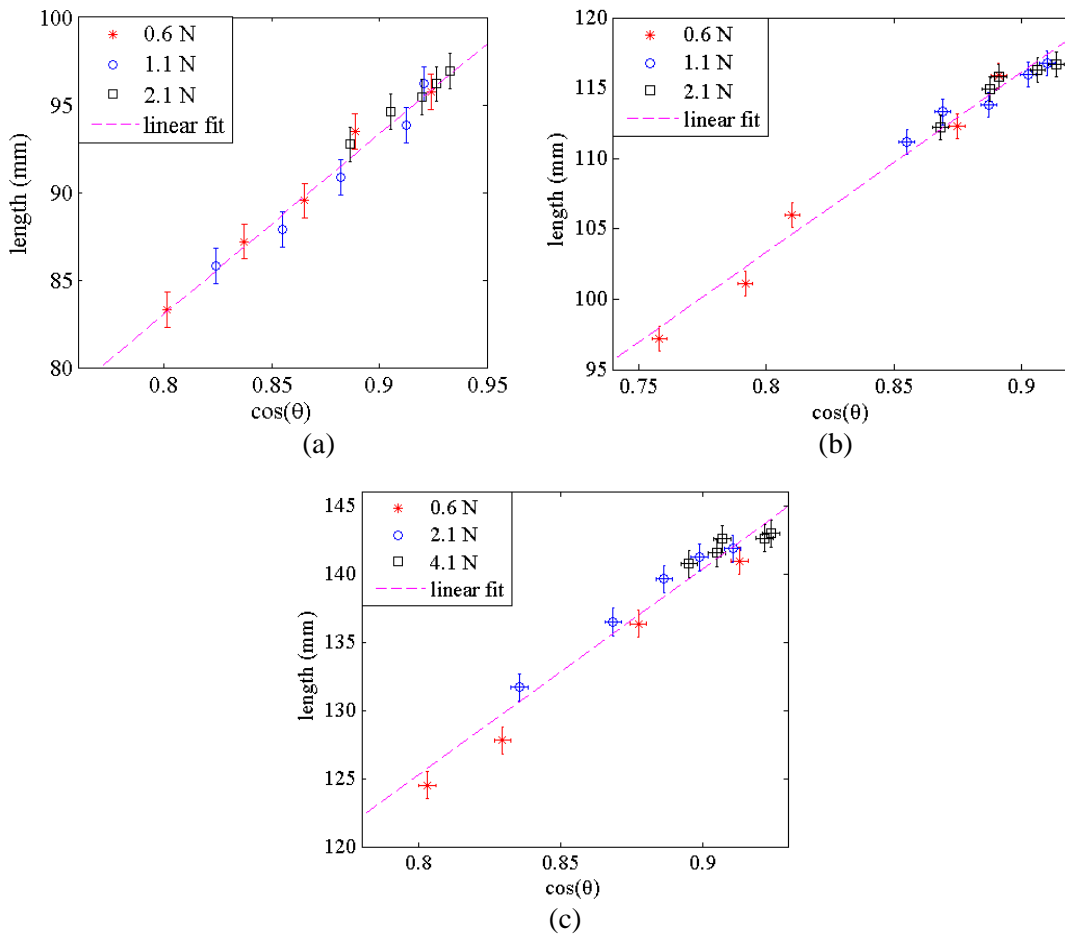


Fig. 9: Length versus cosine of braid angle plot for (a) 97 mm, (b) 117 mm, and (c) 143 mm.

Table I – Best fit straight line results

Initial length of MPAM	L_s	k_1	k_2
97 mm	112 mm	0.92	0.77
117 mm	145 mm	0.88	1.09
143 mm	175 mm	0.86	4.19

1) If the rigid-body pantograph mechanism were to be an accurate model for the contraction of the MPAM, k_1 would be 1.0. As seen from Table 1, and as expected, this is not so. However, the variation from 1.0 is less than 15% for the three tested MPAM. Likewise the value of the intercept, k_2 , would be zero according to the pantograph model given in equation (1). In this case too, the intercept is small compared to the length.

2) The values of k_1 and k_2 deviate more from 1.0 and 0 as the length of the MPAM increases. Although we do not have a definitive theory to explain the deviation in k_1 and k_2 , it is intuitive that the deviation from the rigid body pantograph model will be more if the flexibility and other un-modeled effects are more. As the length increases, the flexibility effects are expected to be more.

We also measured the braid angle at the center of the three different MPAM at different pressures and for two values of loading. This is shown in Fig. 10. It can be seen that the behavior is non-linear as at lower pressures, the braid angle does not change much. It may be noted that a part of this non-linearity is also due to the limitation of measuring the braid angle – we could not measure below +/- 1 degree with the available equipment. A cubic appears to be a good fit

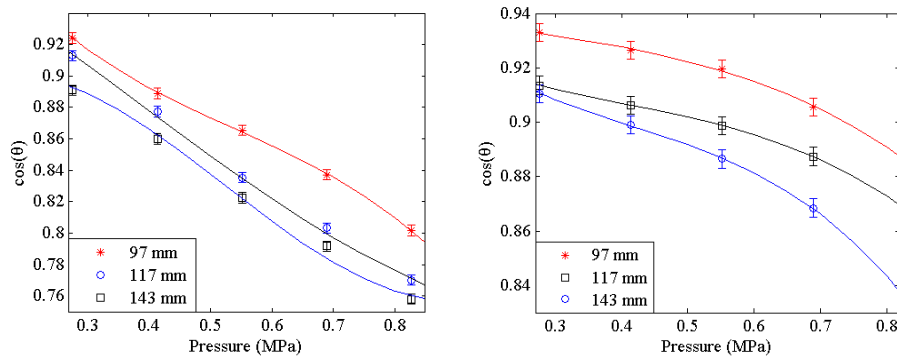


Fig. 10: Cosine θ versus pressure for three MPAMs carrying an end load of 0.6N (left) and 2.1 N (right).

and the equation of cosine of braid angle θ as a function of applied pressure, P for a load of 2.1 N and un-pressurized length of 97 mm is

$$\delta_{97} = -0.1 P^3 + 0.1 P^2 - 0.06 P + 0.94 \quad (3)$$

where δ_{97} denotes cosine θ for initial length of 97 mm. The coefficients of the cubic's for other loads and un-pressurized lengths are given in Table II.

Table II– coefficients of the cubic fit

Load	Cosine of the braid angle	Coefficients			
		P^3	P^2	P	Constant
0.6 N	δ_{97}	-0.6	0.9	-0.71	1.05
	δ_{117}	0.2	-0.2	-0.22	0.98
	δ_{143}	0.8	-1.2	0.34	0.87
2.1 N	δ_{117}	-0.2	0.3	-0.16	0.94
	δ_{143}	-0.4	0.5	-0.31	0.96

Equations (2) and (3) can be combined to obtain the length of an MPAM at an applied pressure. Although the cubics are obtained for two typical load cases, similar experimentally fitted plots can be obtained for other applied loads. Clearly, the un-modeled effects of elasticity of the silicone tube and the braiding strands, friction due to sliding of braids, contact friction between the braid and the silicone tube, density of braids and other un-modeled physical effects will lead to deviation from the purely kinematic and experimental fit given in equations (2) and (3). However, for small MPAMs, as required for our application of actuating the end-effectors in a surgical device, the error from the simplistic rigid-body pantograph mechanism model and the experimentally fitted pressure versus braid angle is expected to be small. This model serves as a good design tool for fabricating the MPAMs and can also be used for a static feed-forward term in the closed loop control of the MPAM, more so since refined sophisticated FEA or analytical models are not available in literature.

IV. CONTROL ARCHITECTURE

One of the difficulties in using PAM is the control of pressure in the pneumatic circuit. To actuate the MPAM developed in this work, we have implemented a control strategy based on sliding mode technique. The block diagram of the controller is shown in Fig.11. A pressure regulating switch, switches on/off the air compressor to maintain the set pressure in the reservoir. The pressure to the pneumatic muscle is supplied through the reservoir and controlled using miniature VSO proportional valves manufactured by Parker Inc [25]. A feedback controller is designed to set the pressure in the pneumatic muscle to a desired value. The controller receives the feedback signal of the measured pressure in the pneumatic muscle and provides the output voltage to drive the proportional valve. The entire instrumentation and controller is implemented on an Arduino Mega 2560 board [26] that is programmed to serially transmit sensor data¹. These transmitted data was captured using a computer for analysis and controller tuning. Since all the controller computations are carried out in the Arduino's processor board itself, there was very little transmission delays and during our experiments we found out that Arduino Mega 2560 board is able to efficiently handle all the instrumentation and control computations when the control loop was set to operate at 1 kHz.

The Arduino Mega 2560 board used in our experiments can output PWM voltages in the range of 0-5 V with maximum current of 40 mA. However, the proportional valves used in our experiments are solenoid valves that are driven by current signals. To drive these valves using Arduino board's 0-5 V voltage output, a current driver circuit was

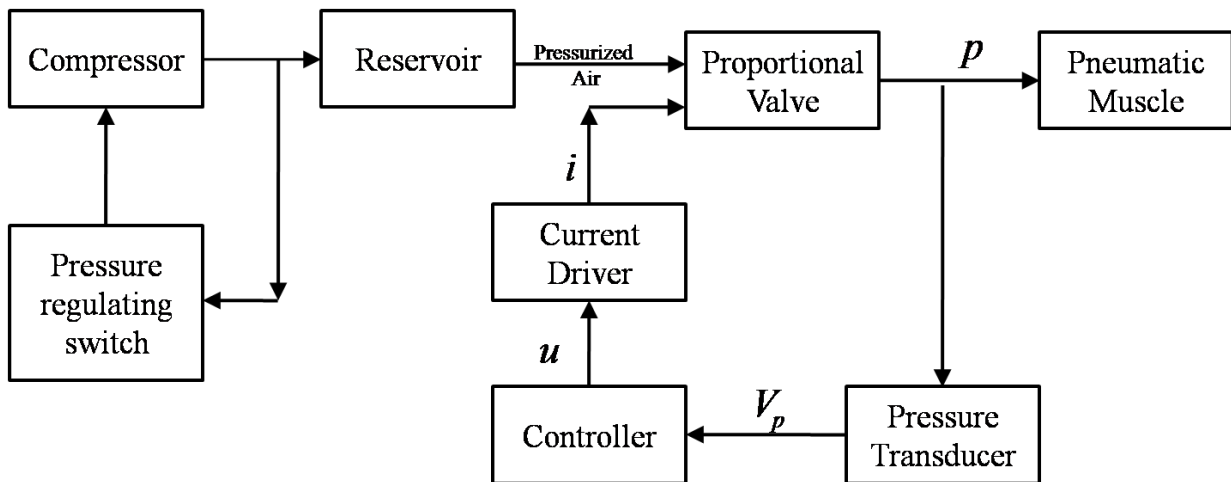


Fig. 11: Control architecture for controlling the developed MPAM.

¹ The Arduino Mega 2560 board also has the advantage of the availability of several PWM channels and these could be useful while designing a surgical device with many actuators. The Arduino Mega 2560 board is also very easy to program.

designed and a PCB for the same was manufactured. The current driver circuit is based on LM 358 IC and draws a maximum current of 1 mA. The circuit diagram of the designed driver circuit is shown in Fig. 12.

A. Controller development

In this sub-section, we present the approach used to develop the controller. Elementary system identification was carried out by giving a voltage step input to the driver circuit and pressure in a 100 mm long pneumatic muscle was noted. We observed from our experiments that the system is fast and has a time constant of ~ 0.09 s and the MPAM system was damped with no overshoot. A first order model of the system based on the step response was obtained and this model was used to design a PID controller using Matlab/SIMULINK [27] simulations. However, we noticed that the controller performance in the actual system was not satisfactory and varied with different step size and back pressure. The reasons for this discrepancy can be attributed to the uncertainties caused by non-linearity in the system. For developing a robust controller that takes care of the uncertainties, a sliding mode control (SMC) scheme [28] was developed. This is described in brief next.

The SMC is formulated based on the error, e , which is the difference between the feedback and set pressure values. If p_d is the desired pressure and p_m the measured pressure, then the error, $e = p_d - p_m$. The desired pressure values are specified by the required contraction according to the static pressure versus contraction maps obtained during characterization of the MPAM or by use of equations (2) and (3).

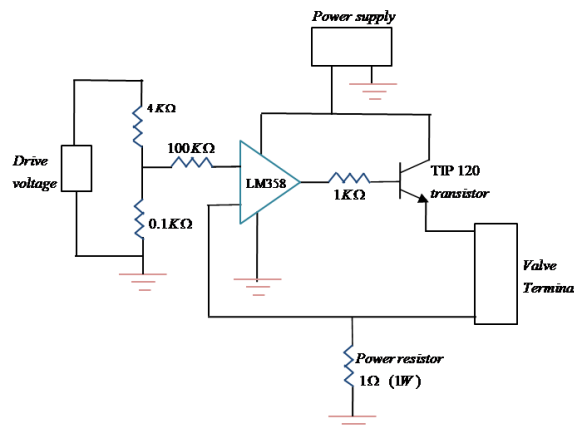


Fig. 12: Current driver circuit for the proportional valve.

The dynamics of the sliding mode controller is defined by the sliding manifold, S , where,

$$S(e,t)=0 \quad (4)$$

Choosing the sliding surface to be a function of error, e and adding an integrator to remove steady state error, we get

$$S = e + K_i \int e dt \quad (5)$$

Now we employ Lyapunov stability theory to determine the stability of the controller [28]. Consider a Lyapunov function, V_L which is positive definite and continuously differentiable.

$$V_L = \frac{1}{2} S^2 \quad (6)$$

Taking derivative with respect to time and substituting from equation (5)

$$\dot{V}_L = S \dot{S}, \quad \text{or} \quad \dot{V}_L = S (\dot{e} + K_i e) \quad (7)$$

Now, consider the first order linear model estimated by open loop experiment. All the unmodeled dynamics and the uncertainties can be lumped into a function $h(p,u)$ and added into the first-order model estimate. The approximate state equation can now be written as:

$$\dot{P} = g(p) + h(p,u) + u \quad (8)$$

Any uncertainty associated with u is also lumped into $h(p,u)$ to make u as linear input to the approximate state equation (8). It is noted from experiments that the uncertainties in the control input are small and do not compromise control authority. Substituting the state equation into Lyapunov function gives,

$$\begin{aligned} \dot{V}_L &= S [\dot{P}_d - \dot{P}_m + K_i e], \quad \text{or} \\ \dot{V}_L &= S [\dot{P}_d - g(p) - h(p,u) - u + K_i e] \end{aligned} \quad (9)$$

Choosing control law to cancel unknown nonlinear functions, we get

$$\begin{aligned} u &= A - \beta \text{sign}(S) \\ \text{where, } A &= -\dot{P}_d + g(p) + h(p,u) - K_i e \end{aligned} \quad (10)$$

For the control system to be stable in the Lyapunov sense, equation (9) has to be negative definite and the following condition should hold for all time, t , i.e., we need

$$\beta \geq A \quad (11)$$

Since all the terms in A are difficult to estimate and characterize, we set β to a large value heuristically to make equation (9) negative definite over a large range of operation. In order to avoid the chatter associated with SMC we implemented the continuous form of the controller given by,

$$u = A - \beta \tanh\left(\frac{S}{\varepsilon}\right) \quad (12)$$

B. Controller validation

We validated and characterized the performance of the robust controller derived in the previous section to set the desired pressure in the MPAM. A step input to set the pressure in MPAM to 0.55 MPa (80 psi) is given to the controller. Figure 13(a) and figure 13(b) shows the step response of the controller for two different β values 120 and 150. The time constant of the controller response is found to be ~ 0.06 s for the low gain. By choosing β to be 150, the response time can be further reduced to 0.01 s with a small increase in overshoot ($\sim 7\%$). We note that the controller response time will be limited by the response time of the proportional valves, which is in the order of few milliseconds. We also note that any small leak in the pneumatic circuit conditions the flow and aids in obtaining high control accuracy with a small sacrifice of response time.

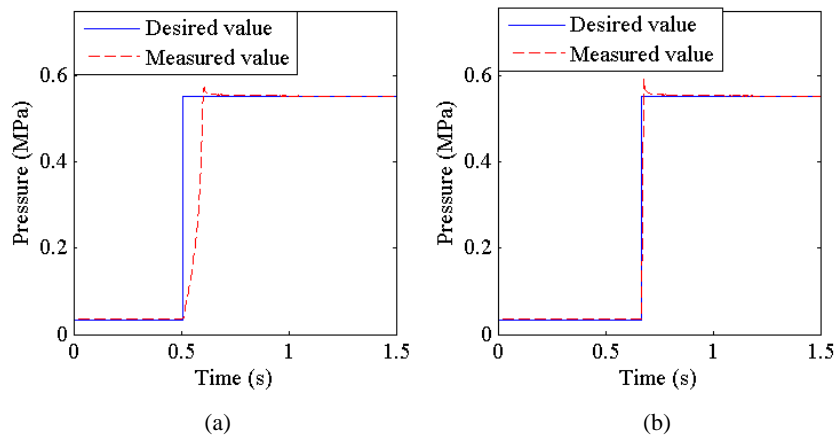


Fig 13: Controller response for gain (a) 120 and gain (b) 150.

V. INITIAL DESIGN AND EXPERIMENTS WITH A MPAM BASED SURGICAL TOOL

Once the MPAM and the controller was designed and characterized, we next developed concepts for an articulated endoscope. This section describes initial attempts and the work is continuing. Figure 14 (a) shows the CAD model of the prototyped surgical device. The device consists of 12 mm diameter spacer discs with three 120° spaced peripheral holes. The three MPAM can be independently controlled by applying required pressure and the tip of the prototype can be positioned in 3D space. The MPAMs are inserted through the peripheral holes of the closely spaced spacer discs. The diameter of the peripheral holes is 2.2 mm to allow for easy inserting and small expansion during actuation of MPAMs. A 4 mm hole in the center of each spacer disc relieves space for inserting fiber optic camera and other surgical tools such as like scissors or a biopsy tool. For the prototype, the spacer discs were manufactured using a rapid prototyping. Figure 14 (b) shows snapshots of the endoscopic surgical device as the air pressure is applied to the MPAMs. These snapshots are extracted from a video showing motion of the prototype endoscope.

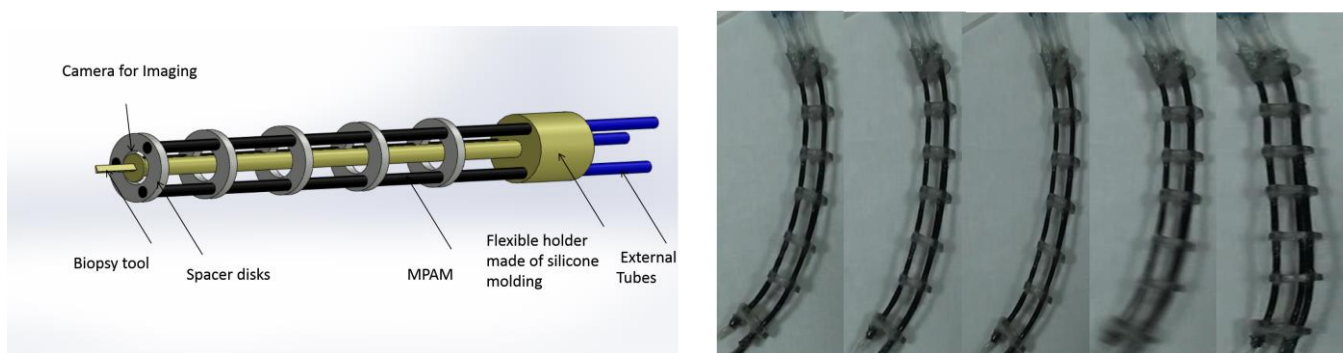


Fig 14: (a) CAD illustration of the prototype, (b) Snapshots showing the rotational motion of the endoscopic surgical device.

VI. CONCLUSION

This paper deals with the development and modeling of efficient and reliable miniature pneumatic actuators that can be used for actuation in minimally invasive surgical tools. The paper also presents control of these MPAMs. The characterization of the fabricated MPAM showed that the actuators can provide a reasonably large force (~5 N) when operating at a maximum pressure of 1 MPa. An initial model based purely on kinematics and fitting of experimental data is shown to be accurate within 18% and we plan to use this model for model-based control in future. A robust

control scheme based on sliding manifold is derived for controlling pressure in the MPAMs. The controller is robust against uncertainties and has fast response (~ 0.01 s). We have also proposed an endoscopic surgical tool actuated by MPAMs. Future research will focus on improving the proposed endoscopic surgical device with continuous tracking control and manipulation capability.

ACKNOWLEDGEMENT

This work was financially supported by the Robert Bosch Centre for Cyber Physical Systems (RBCCPS) at the Indian Institute of Science, Bangalore. We would like to thank Professor G. K. Ananthasuresh for his inputs and permitting us to use the facilities at the M2D2 lab, IISc. We also appreciate the help of Raghavan and his team at the Electrical & Allied Products, Bangalore for providing customized braid used in this work.

REFERENCES

- [1] Della Flora, E., Wilson, T. G., Martin, I. J., O'Rourke, N. A., and Maddern, G., 2008, "Review of Natural Orifice Transluminal Endoscopic Surgery (Notes) for Intra-Abdominal Surgery: Experimental Models, Techniques and Applicability to the Clinical Setting," *Annals of surgery*, 247(4), pp. 583-602.
- [2] Chou, C.-P., and Hannaford, B., 1996, "Measurement and Modeling of McKibben Pneumatic Artificial Muscles," *Robotics and Automation, IEEE Transactions on*, 12(1), pp. 90-102.
- [3] De Volder, M., Moers, A., and Reynaerts, D., 2011, "Fabrication and Control of Miniature McKibben Actuators," *Sensors and Actuators A: Physical*, 166(1), pp. 111-116.
- [4] Tondu, B., and Lopez, P., 2000, "Modeling and Control of McKibben Artificial Muscle Robot Actuators," *IEEE Control Systems Magazine*, 20(2), pp. 15-38.
- [5] Trivedi, D., Rahn, C. D., Kier, W. M., and Walker, I. D., 2008, "Soft Robotics: Biological Inspiration, State of the Art, and Future Research," *Applied Bionics and Biomechanics*, 5(3), pp. 99-117.
- [6] Ikuta, K., Nokata, M., and Aritomi, S., 1994, "Biomedical Micro Robots Driven by Miniature Cybernetic Actuator," eds., pp. 263-268.
- [7] Kai, X., Goldman, R. E., Jienan, D., Allen, P. K., Fowler, D. L., and Simaan, N., 2009, "System Design of an Insertable Robotic Effector Platform for Single Port Access (Spa) Surgery," eds., pp. 5546-5552.
- [8] Szewczyk, J., De Sars, V., Bidaud, P., and Dumont, G., 2001, *Experimental Robotics VII*, Springer, An Active Tubular Polyarticulated Micro-System for Flexible Endoscope.
- [9] Degani, A., Choset, H., Wolf, A., and Zenati, M. A., 2006, "Highly Articulated Robotic Probe for Minimally Invasive Surgery," eds., Piscataway, NJ, USA, pp. 4167-72.

- [10] Slatkin, A. B., Burdick, J., and Grundfest, W., 1995, "The Development of a Robotic Endoscope," eds., 2, pp. 162-171.
- [11] Webster, R. J., and Jones, B. A., 2010, "Design and Kinematic Modeling of Constant Curvature Continuum Robots: A Review," *The International Journal of Robotics Research*, 29(13), pp. 1661-1683.
- [12] Jianzhong, S., Payne, C. J., Clark, J., Noonan, D. P., Ka-Wai, K., Darzi, A., and Guang-Zhong, Y., 2012, "Design of a Multitasking Robotic Platform with Flexible Arms and Articulated Head for Minimally Invasive Surgery," eds., Piscataway, NJ, USA, pp. 1988-93.
- [13] Kornbluh, R., Pelrine, R., Eckerle, J., and Joseph, J., 1998, "Electrostrictive Polymer Artificial Muscle Actuators," eds., 3, pp. 2147-2154.
- [14] Moers, A., De Volder, M., and Reynaerts, D., 2012, "Integrated High Pressure Microhydraulic Actuation and Control for Surgical Instruments," *Biomedical microdevices*, 14(4), pp. 699-708.
- [15] Tondu, B., 2012, "Modelling of the Mckibben Artificial Muscle: A Review," *Journal of Intelligent Material Systems and Structures*, 23(3), pp. 225-253.
- [16] Klute, G. K., and Hannaford, B., 1998, "Fatigue Characteristics of Mckibben Artificial Muscle Actuators," eds., 3, pp. 1776-1781.
- [17] Liu, W., and Rahn, C. R., 2003, "Fiber-Reinforced Membrane Models of Mckibben Actuators," *Journal of Applied Mechanics*, 70(6), pp. 853.
- [18] Ramasamy, R., Juhari, M. R., Mamat, M., Yaacob, S., Nasir, N. M., and Sugisaka, M., 2005, "An Application of Finite Element Modelling to Pneumatic Artificial Muscle," *American Journal of Applied Sciences*, 2(11), pp. 1504.
- [19] Zhou, B., Accorsi, M., and Leonard, J., 2004, "A New Finite Element for Modeling Pneumatic Muscle Actuators," *Computers & structures*, 82(11), pp. 845-856.
- [20] De Volder, M., Coosemans, J., Puers, R., and Reynaerts, D., 2008, "Characterization and Control of a Pneumatic Microactuator with an Integrated Inductive Position Sensor," *Sensors and Actuators A: Physical*, 141(1), pp. 192-200.
- [21] Woods, B. K., Choi, Y.-T., Kothera, C. S., and Wereley, N. M., 2013, "Control System Development for Pneumatic Artificial Muscle-Driven Active Rotor Systems," *Journal of Guidance, Control, and Dynamics*, 36(4), pp. 1177-1185.
- [22] Kothera, C. S., Jangid, M., Sirohi, J., and Wereley, N. M., 2009, "Experimental Characterization and Static Modeling of Mckibben Actuators," *Journal of Mechanical Design*, 131(9), pp. 091010.
- [23] Nagaraj, B., Pandiyan, R., and Ghosal, A., 2009, "Kinematics of Pantograph Masts," *Mechanism and Machine Theory*, 44(4), pp. 822-834.
- [24] Abràmoff, M. D., Magalhães, P. J., and Ram, S. J., 2004, "Image Processing with Imagej," *Biophotonics international*, 11(7), pp. 36-42.
- [25] Parker, 2013, "Miniature Valves", Available: <http://ph.parker.com/us/12051/en/vso-miniature-proportional-valve> (Date accessed 11/5/2013).
- [26] Arduino, 2012 "An Open-Source Electronics Prototyping Platform", Available: <http://www.arduino.cc> (Date accessed 11/5/2013).

[27] Matlab, Version 7.12.0 (R2012a), 2012, The MathWorks Inc., Natick, Massachusetts.

[28] Khalil, H. K., 1992, *Nonlinear Systems*, Maxwell Macmillan,